Shahid Bahonar University of Kerman

Biomechanism and Bioenergy Research

Online ISSN: 2821-1855
Homepage: https://bbr.uk.ac.ir

Iranian Society of Agricultural Machinery Engineering and Mechanization

Non-Destructive Authentication of Rice Varieties Using Hyperspectral Imaging and Machine Learning

Esmat Kishani Farahani [1]✉, **Seyedehsamaneh Shojaielangari** [2]

[1] Information Technology and Intelligent Systems Group, Department of Electrical Engineering and Information Technology, Iranian Research Organization for Science and Technology (IROST), Tehran, Iran.

[2] Biomedical Engineering Group, Department of Electrical Engineering and Information Technology, Iranian Research Organization for Science and Technology (IROST), Tehran, Iran.

✉ Corresponding author: e.kishani@irost.ir

ARTICLE INFO

Article type:

Research Article

Article history:

Received 11 September 2025

Received in revised form 28 October 2025

Accepted 16 December 2025

Available Online 31 March 2026

Keywords:

Hyperspectral Imaging, LSTM, SVM, 1D-CNN, Feature Extraction, Rice Variety Identification.

ABSTRACT

This study develops a non-destructive method for authenticating four commercial rice varieties: Sargol, Domsiyah, AliKazemi, and Aria-Paria, by integrating hyperspectral imaging (HSI) with machine learning. Hyperspectral data in the visible–near infrared range (400–950 nm) were acquired from 4,305 individual rice grains. Effective preprocessing mitigated initial anisotropic spatial sampling by resizing images to achieve isotropic resolution, preventing grain loss during segmentation. Two analytical strategies were investigated: one relying on handcrafted features and another directly exploiting reduced spectral profiles as sequential data. Comparative evaluation showed that models trained on sequential spectral information consistently outperformed feature-based methods. Among the evaluated classifiers, a Support Vector Machine (SVM) achieved the highest classification accuracy of 92.62%, exceeding both classical machine learning models and deep learning approaches, including Long Short-Term Memory (LSTM) networks, one-dimensional Convolutional Neural Networks (1D-CNNs), and a hybrid CNN-LSTM architecture. The proposed HSI–SVM framework demonstrates strong potential for accurate rice variety authentication and offers practical applicability in quality control and supply chain monitoring.

Cite this article: Kishani Farahani, E., & Shojaielangari, S (2026). Non-Destructive Authentication of Rice Varieties Using Hyperspectral Imaging and Machine Learning. *Biomechanism and Bioenergy Research*, *5*(1), 1-19. https://doi.org/10.22103/bbr.2026.26384.1142

Publisher: Shahid Bahonar University of Kerman
DOI: https://doi.org/10.22103/bbr.2026.26384.1142

INTRODUCTION

Rice (Oryza sativa L.) is a major global staple crop, providing a primary food source for over half the global population (Prova, 2025). Ensuring its quality and authenticity is therefore critical for food security, consumer safety, and economic stability in many regions (Feng et al., 2021). In commercial markets, accurate varietal identification is essential to prevent adulteration, maintain brand integrity, and guarantee fair pricing (Fabiyi et al., 2020; Kiratiratanapruk et al., 2020; Komal et al., 2022). Traditional methods for distinguishing rice varieties have predominantly relied on visual inspection by human experts or laboratory-based chemical analyses. However, these approaches are often subjective, time-consuming, and destructive, making them unsuitable for rapid, large-scale quality control in modern agricultural supply chains (Kang et al., 2024; Qiu et al., 2018).

In recent years, hyperspectral imaging (HSI) has emerged as a powerful, non-destructive analytical technique that combines the principles of spectroscopy and digital imaging. Unlike conventional RGB cameras, HSI captures a contiguous spectrum for each pixel, generating a three-dimensional data cube that contains both spatial and spectral information. This rich data can be related to a sample's chemical and physical properties, making HSI particularly well-suited for agricultural product assessment (Kang et al., 2024; Qiu et al., 2018). Its application has been explored for quality evaluation of various grains, fruits, and vegetables (Ahmed et al., 2025; Feng et al., 2021).

The analytical potential of hyperspectral imaging (HSI) data for rice analysis is fully realized through machine learning algorithms, which address inherent challenges such as spectral band redundancy, limited training samples, and non-linear spatial–spectral relationships in rice grain measurements. By leveraging feature extraction, dimensionality reduction, and pattern recognition techniques, machine learning models enable efficient exploitation of high-dimensional spectral data while preserving subtle yet discriminative information associated with varietal differences. Both classical machine learning approaches and deep learning architectures have been employed to capture complex spectral variations arising from differences in rice grain composition, structure, and surface characteristics, thereby enhancing the robustness and generalization performance of rice variety classification models.

The study by Qiu et al. explores the feasibility of using hyperspectral imaging combined with convolutional neural networks (CNNs) for non-destructive identification of single rice seeds from four varieties (Qiu et al., 2018). Hyperspectral images were acquired in two spectral ranges: 380–1030 nm and 874–1734 nm, with relevant spectral data extracted from 441–948 nm (Range 1) and 975–1646 nm (Range 2). Classification models, including K-nearest neighbors (KNN), support vector machines (SVM), and CNN, were developed using varying training sample sizes (100 to 3000). Models in Range 2 slightly outperformed those in Range 1, with overall accuracy improving as sample size increased but plateauing at higher volumes. The CNN model consistently surpassed KNN and SVM in most scenarios, demonstrating its effectiveness for spectral data analysis and validating HSI-CNN as a promising approach for rice variety identification, though the authors recommend future research on additional varieties to broaden applicability

Kang et al. utilized fluorescence hyperspectral imaging (FHSI) in the 475–1000 nm wavelength rage combined with machine learning for the classification of five similar-looking rice varieties (Kang et al., 2024). Fluorescence hyperspectral data from rice samples were preprocessed with first-order derivative (FD) to mitigate background and baseline drift effects. Principal component analysis (PCA) and t-distributed stochastic neighbor embedding (t-SNE) were applied for feature reduction and 3D visualization, revealing distinct clustering among varieties. Classification models, including partial least squares discriminant analysis (PLS-DA),

back-propagation neural network (BP), and random forest (RF), were developed. The method yielded superior performance, with accuracies of 99.8% and 95.3% on the training and test sets, respectively, confirming the feasibility of FHSI-based machine learning for non-destructive rice variety identification.

Jin et al. proposed a multi-dimensional fusion CNN for accurate, non-destructive classification of rice seed varieties using HSI in the 900–1700 nm near-infrared range (Jin et al., 2025). The method addresses limitations in traditional HSI approaches, such as reliance on hand-engineered features and challenges in capturing both spatial and spectral dimensions, by integrating a spatial-spectral fusion module that combines 1D spectral convolutions for wavelength-wise feature extraction with 2D spatial convolutions for morphological pattern recognition. The proposed model achieved a mean classification accuracy of 98.5%, representing an improvement of up to 11.9% compared with the SVM baseline. These results highlight the model's capability to effectively exploit fused spatio-spectral representations for discriminating subtle varietal differences. The findings demonstrate the effectiveness of deep learning–based fusion strategies in enhancing HSI-driven rice variety identification, with potential applications in precision agriculture and seed quality assessment.

Despite recent advances, reliable classification of agricultural products that exhibit high visual and spectral similarity remains a significant challenge, particularly under practical acquisition conditions. This study addresses this gap by investigating the integration of hyperspectral imaging and machine learning for the discrimination of four commercially rice varieties. Unlike many existing studies conducted under tightly controlled laboratory settings, the proposed approach is designed to operate under conditions that more closely reflect real-world scenarios, including variations in grain orientation during image acquisition, and natural heterogeneity in grain size.

The primary contributions of this work are threefold. First, a robust and computationally efficient image analysis pipeline is developed to segment individual rice grains from low-spatial-resolution HSI data without imposing constraints on grain orientation, thereby supporting fast implementation. Second, discriminative spectral information is extracted and analyzed to characterize subtle varietal differences while preserving the integrity of the non-destructive assessment. Third, the performance of a diverse set of machine learning classifiers including SVM, RF, Multinomial Logistic Regression (MLR), Decision Tree (DT), Gradient Boosting (GB) is systematically evaluated and compared with that of deep learning models including CNNs, long short-term memory (LSTM) networks, and a hybrid CNN-LSTM architecture.

By emphasizing robustness, speed, and minimal assumptions about sample preparation, this study establishes an effective non-destructive framework for rice varietal authentication that is well suited for real-time and commercial deployment. The proposed methodology has the potential to enhance quality control, support supply chain transparency, and facilitate large-scale varietal verification within the rice industry.

The remainder of the paper is structured as follows. Section 2 describes the materials and methods, including sample preparation, hyperspectral image acquisition, spectral preprocessing, model architectures, and the experimental setup. Section 3 presents the results, followed by discussion in Section 4. Finally, Section 5 concludes the study.

MATERIALS AND METHODS

Sample Preparation

Four commercial rice varieties were selected for this study: three Iranian cultivars (Sargol, Domsiah, and Alikazemi) and one Pakistani cultivar (Aria-Paria). A 120-gram sample of each variety was procured from a reliable supplier. The samples are shown in Figure 1.

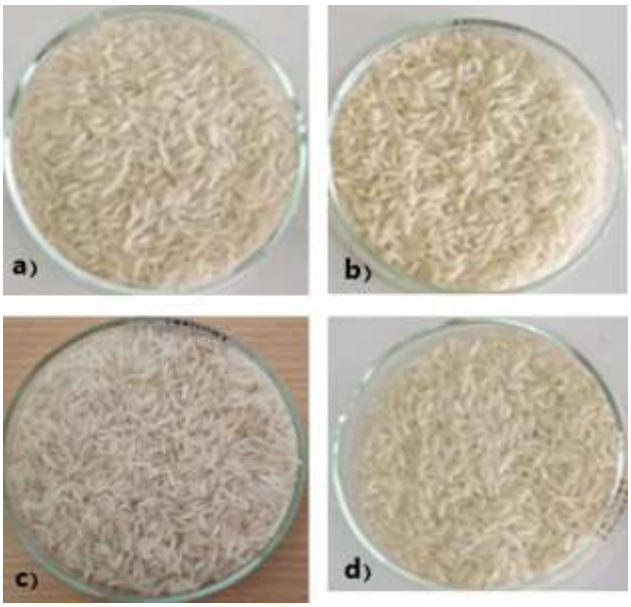

Figure 1. Image of four rice varieties. a) Sargol, b) Domsiyah, c) Aira-paria, and d) Alikazemi.

Hyperspectral Image Acquisition

A line-scanning hyperspectral imaging system (a desktop model by HYSYIM Company) was used for image acquisition. The system comprised a hyperspectral camera, a scanning stage controlled by a PC, and three halogen lamps for illumination. The camera operates in the visible to near-infrared range of 400–950 nm with 993 spectral bands. The spatial resolution is 210 micrometers in the scanning direction and 1 mm in the vertical direction.

The imaging procedure was as follows. First, the halogen lamps were switched on and allowed to stabilize for 2.5 minutes to ensure consistent illumination. The system was then calibrated using white and black reference standards. Subsequently, for each imaging round, rice grains from a single variety were randomly selected and arranged in a grid pattern on the scanning platform (Figure 2).

During image acquisition, the scanner moved smoothly to capture the first image. After this capture, the scanner returned to its start position at a higher speed. This rapid return motion caused slight rotations, tilts, or displacements of the grains, effectively changing their orientation. A second image was captured to obtain these alternative views of the grains, thereby expanding the dataset with multiple perspectives. Following a second return of the scanner, a third and final image was captured. In total, three images were acquired for each unique set of grains on the scanner.

For each of the four rice varieties, two distinct sets of grains were prepared. Consequently, six images were captured per variety (2 sets × 3 images/set). With each image containing approximately 180 rice grains, this resulted in a total of about 1080 grain samples per variety (6 images × 180 grains). This entire procedure was repeated for all four varieties.

a) b)

Figure 2. a) Hyperspectral imaging system; b) Arrangement of rice grains on the scanner.

Data Preprocessing and Spectral Data Extraction

A hyperspectral data processing pipeline was designed to overcome the challenge of low spatial

resolution and extract clean spectral signatures from individual rice grains. The procedure consisted of four main stages: spatial enhancement, image preprocessing, segmentation, and spectral extraction.

First, to address the insufficient native spatial resolution of the hyperspectral images (approximately 1 pixel/mm), each spectral band was resized from 472 × 200 to 472 × 1000 pixels using bilinear interpolation. This spatial enhancement step was employed to better define the boundaries of rice grains.

Following spatial enhancement, a pseudo-RGB image was constructed for segmentation purposes by extracting and combining bands centered at 650 nm (red), 550 nm (green), and 450 nm (blue). This image then was converted to grayscale and processed using Contrast Limited Adaptive Histogram Equalization (CLAHE) to improve local contrast (Zuiderveld, 1994). CLAHE has been widely adopted in recent agricultural and food imaging studies to improve object–background separability under non-uniform illumination conditions (Bajait & Malarvizhi, 2024; Kurniawan & Sunardi, 2025). Following CLAHE, a linear contrast adjustment was further applied to intensify the distinction between the grains and the background.

The third stage involved segmenting the individual rice grains using the Watershed algorithm (Beucher & Meyer, 2018). The enhanced grayscale image was initially binarized using Otsu's thresholding method, followed by morphological opening to eliminate small noise artifacts. The Watershed transformation was subsequently applied to the distance-transformed binary image, enabling precise separation of adjacent grains and the assignment of a unique label to each segmented object. Comparative results of the processing pipeline pre- and post-enhancement are presented in Figure 3 and Figure 4, respectively

Finally, for each labeled region identified by the Watershed algorithm, the corresponding spectral data was extracted from the enhanced hyperspectral cube. The reflectance values of all pixels belonging to a single grain were averaged to produce a representative spectrum for that grain. Each resulting average spectrum was then smoothed using a Savitzky-Golay filter to reduce high-frequency noise. This comprehensive pipeline resulted in a final dataset of 4,305 samples, each defined by 993 spectral features (Savitzky & Golay, 1964).

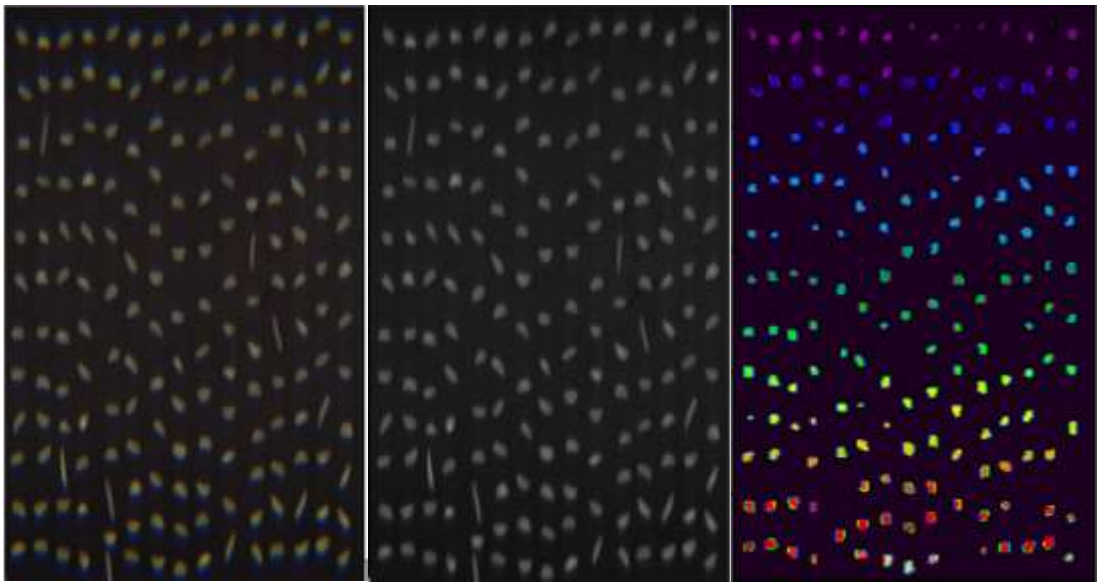

a) b) c)

Figure 3. Before spatial enhancement: a) RGB image; b) grayscale image; c) segmented image.

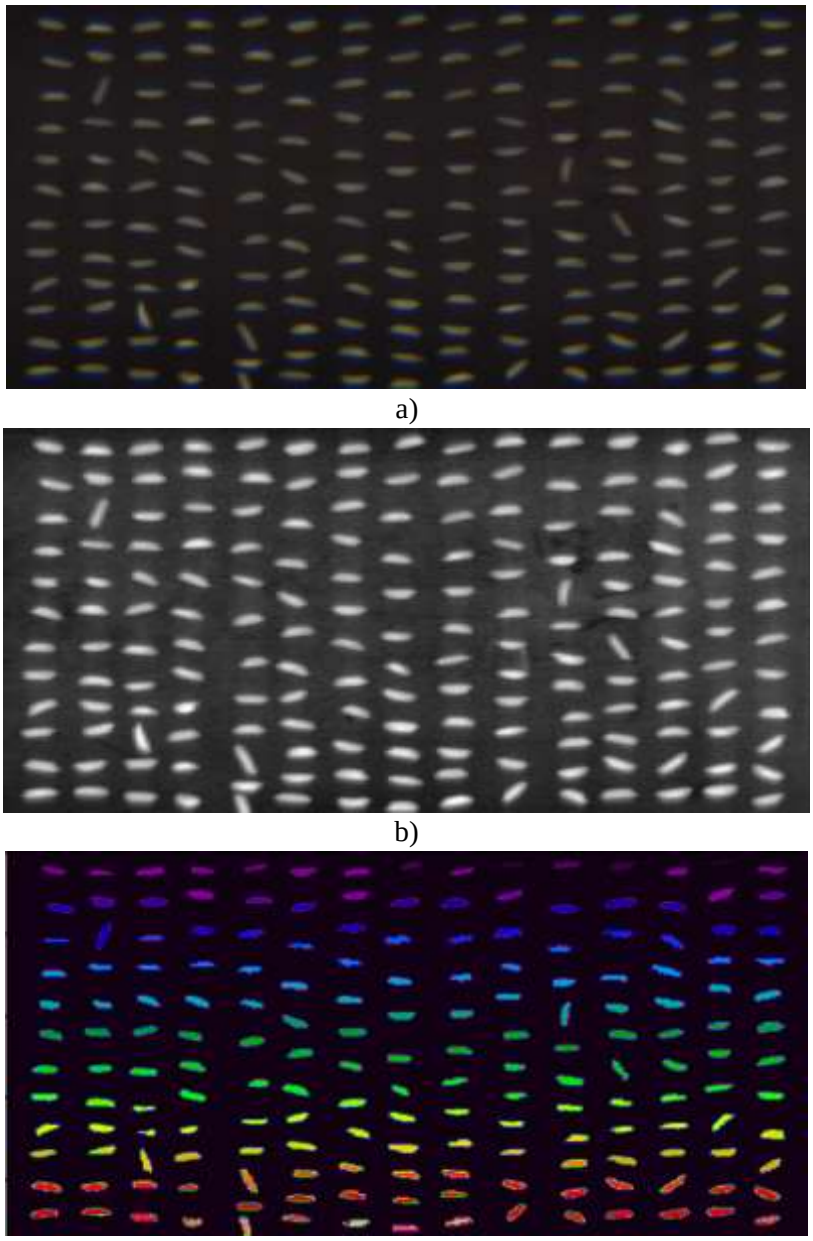

Figure 4. After spatial enhancement: a) RGB image; b) grayscale image; c) segmented image.

Data Visualization

More than four thousand spectral profiles were obtained from the previous step. Plotting all spectra in a single figure made them indistinguishable. To better understand the variation in reflectance spectra within each rice variety, K-means clustering (Hartigan & Wong, 1979; Saber et al., 2025) was applied. This method reveals the diversity of reflectance spectra present in each variety. Ten clusters were considered for each rice variety; this number was determined through trial and error to provide a clear representation of the spectral variation within each variety. The centers of the ten clusters for each variety are plotted in Figure 5. Additionally, the cluster centers for all rice varieties are shown together in Figure 6.

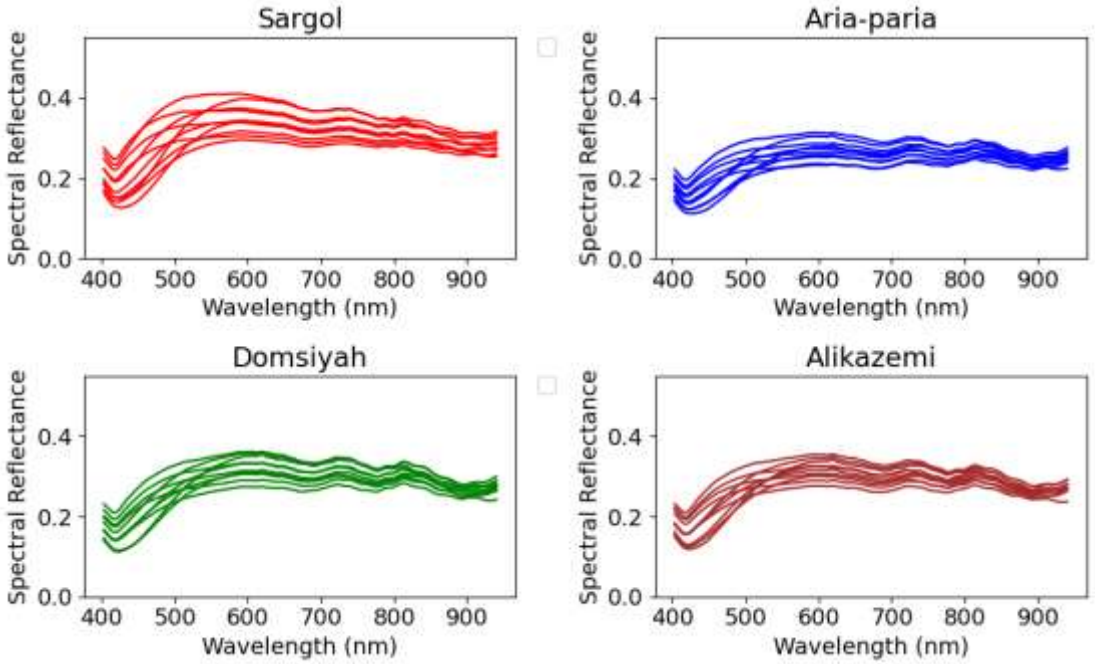

Figure 5. Cluster centers for the 10 clusters of each rice variety.

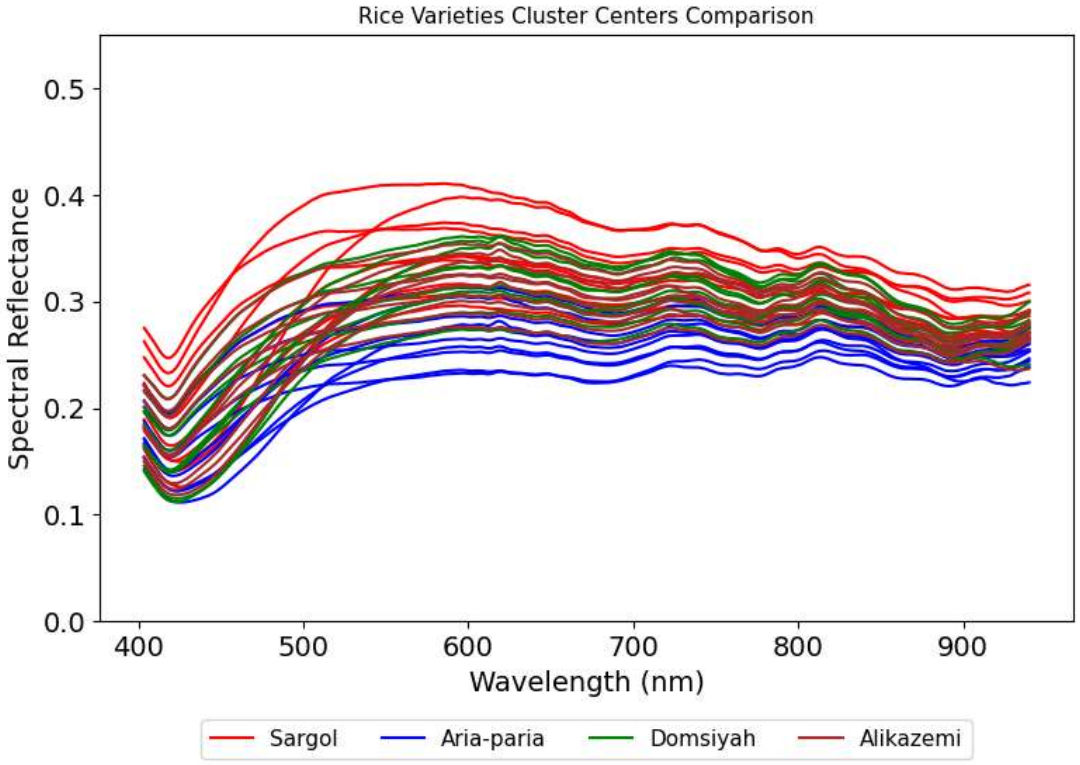

Figure 6. Cluster centers of the 10 clusters for all rice varieties. Each color represents the cluster centers of a specific rice variety.

Feature Extraction

To reduce the high dimensionality of the dataset, a multi-domain feature extraction approach was implemented. This approach captures both statistical and spectral characteristics of the input spectra, resulting in an enriched feature set that enhances model performance and interpretability.

A total of 27 distinct features were extracted from each spectral sample, divided into the following five groups:

Statistical features (10 features): Arithmetic mean, median, standard deviation, variance, peak-to-peak range, interquartile range, skewness (third moment), kurtosis (fourth moment), 25th percentile, and 75th percentile. These features characterize the overall intensity distribution and shape of the spectral profiles, providing fundamental statistical descriptors of spectral variations across different classes.

Spectral peak characteristics (4 features): Peak count, mean peak height, standard deviation of peak heights, and maximum peak height. Peaks were identified as significant local maxima (height > 0.1, minimum peak distance = 5). These features capture critical information about prominent spectral signatures, which often correspond to specific chemical or physical properties of the samples.

Spectral shape descriptors (5 features): Area under the curve (calculated via trapezoidal integration), wavelength of maximum intensity, the difference between maximum and minimum intensities, and the mean and standard deviation of the first derivatives. These descriptors quantify the global morphology of the spectral curves, encoding information about absorption patterns and spectral continuity (Rinnan et al., 2009).

Frequency domain features (3 features): Mean of Fast Fourier Transform (FFT) magnitudes, standard deviation of FFT magnitudes, and the position of the maximum FFT magnitude. This analysis reveals periodic patterns and noise characteristics not apparent in the original spectral domain (Rao et al., 2010).

Signal quality and local variation metrics (5 features): Signal-to-noise ratio (SNR), mean absolute difference between adjacent points, mean of rolling means, standard deviation of rolling means, and mean of rolling standard deviations (window size = 5 for all rolling calculations). These metrics assess data quality and capture local spectral variations that may indicate subtle class-specific patterns.

Classical Classification Models

Five classical machine learning models (SVM (Cortes & Vapnik, 1995), RF (Breiman, 2001), MLR (Sperandei, 2014), DT (Breiman et al., 2017), and GB (Friedman, 2002)) were employed for classification (Géron, 2022). The SVM classifier was implemented with a Radial Basis Function (RBF) kernel, which projects input features into a high-dimensional space to construct optimal hyperplanes for class separation. The RBF kernel effectively handles non-linear decision boundaries by computing the similarity between data points based on their Euclidean distance. Key parameters included a regularization parameter C=100 to balance margin maximization and classification error, and gamma='scale', which automatically sets the kernel coefficient.

The RF ensemble method was configured with 200 decision trees to enhance predictive stability through bootstrap aggregation and feature randomization. Each tree was grown to its full depth without pre-pruning constraints, allowing individual trees to capture complex patterns while ensemble averaging mitigated overfitting. The model used the Gini impurity criterion for node splitting. RF's inherent feature importance calculation provided insights into spectral feature contributions, while out-of-bag error estimation offered an internal validation mechanism.

MLR with L2 regularization (Ridge regression) was implemented using the limited-memory Broyden–Fletcher–Goldfarb–Shanno (L-BFGS) solver (Liu & Nocedal, 1989), which efficiently handles multiclass problems and is optimized for L2-penalized optimization. The model featured an increased maximum iteration limit (2000) to ensure convergence in the high-dimensional feature space. Class weights were balanced

automatically to address potential dataset skewness, and the multiclass strategy employed a one-vs-rest approach, which trains a separate binary classifier for each class against all others.

The DT classifier was implemented with the Gini impurity criterion for node splitting and was grown without depth restrictions to capture complex decision boundaries. The model featured balanced class weights and employed cost-complexity pruning to prevent overfitting. The splitting strategy considered all available features at each node, with a minimum of two samples required for a leaf node and one sample for a split. While prone to overfitting, the model's transparent decision pathways provided valuable interpretability.

The GB model employed sequential ensemble learning with 300 estimators, using the log loss function for multiclass classification. A learning rate of 0.1 controlled the contribution of each weak learner, and the tree depth was limited to three levels to constrain model complexity and enhance generalization. The subsampling fraction was set to 1.0 (using all samples), and all features were considered for each boosting iteration. GB's stagewise additive modeling approach progressively reduced residual errors through optimized tree sequences.

Deep Learning Models

Classification of rice varieties was also performed using four deep learning models: a 1D-CNN, two LSTM variants, and a stacked CNN-LSTM model (Zhang et al., 2023). Prior to model training, dimensionality reduction was applied to the spectral profiles to preserve the sequential structure of the data while significantly reducing computational load. Specifically, one out of every 20 spectral bands was selected for model input.

1D-CNN

A 1D-CNN was employed for feature extraction and spectral classification, as it effectively learns discriminative features by modeling local dependencies between neighboring wavelength bands (Kiranyaz et al., 2019). The network receives a one-dimensional spectral vector as input with a single channel corresponding to the reflectance values across wavelength bands. The feature extraction module consists of two convolutional blocks. In the first block, a 1D convolution layer with 32 filters and a kernel size of 7 is applied using same padding, followed by batch normalization, a ReLU activation function, and max pooling with a pooling size of 2 to capture local spectral patterns and reduce the spectral dimensionality. The second convolutional block applies 64 filters with a kernel size of 3, followed by batch normalization and ReLU activation, and uses adaptive average pooling to produce a fixed-length feature representation independent of the input spectral length. The extracted features are then passed to a classification module composed of a fully connected layer with 32 neurons and ReLU activation, followed by dropout with a rate of 0.3 to mitigate overfitting. The final output layer maps the learned features to the target classes, with class probabilities implicitly learned using the softmax function through the cross-entropy loss. The model was trained using the Adam optimizer with a learning rate of 0.0005 and optimized using categorical cross-entropy loss.

LSTM

LSTM is a type of recurrent neural network designed to capture long-term dependencies in sequential data by controlling information flow through gating mechanisms, making it well-suited for sequential analysis (Hochreiter & Schmidhuber, 1997). Two LSTM networks were employed to model the sequential nature of the hyperspectral signatures.

The first architecture consisted of a single LSTM layer with 98 hidden units, chosen to capture long-range dependencies within the data. This was followed by a fully connected linear layer that mapped the final hidden state to the output layer, which used a softmax activation function for multi-class classification corresponding to the four rice varieties. The model was trained using the Adam optimizer with

a learning rate of 0.0005 and a cross-entropy loss function. To prevent overfitting, early stopping was implemented with a patience of 10 epochs, monitoring validation loss as the primary stopping criterion. Training halted if validation loss failed to improve for 10 consecutive epochs, ensuring model generalization without excessive memorization of training spectral signatures. The training was configured for a maximum of 100 epochs with a batch size of 20.

The second architecture is a 2-layer LSTM network. The network receives preprocessed spectral vectors as input and first passes them through a 64-unit LSTM layer, followed by batch normalization and a dropout rate of 0.3 to stabilize training and reduce overfitting. The output is then fed into a second 32-unit LSTM layer, which captures sequential dependencies across the spectral bands, again followed by batch normalization and dropout. The sequential features are then mapped through a fully connected dense layer with 32 neurons and ReLU activation, with an additional dropout of 0.2, before being projected to the output layer, which consists of a number of neurons equal to the classes and employs a softmax activation function to produce class probabilities. The model is trained using the Adam optimizer with a learning rate of 0.005, minimizing the categorical cross-entropy loss, and monitored using early stopping and learning rate reduction based on validation performance. This architecture effectively combines sequential feature learning and regularization to achieve robust classification on spectral data.

CNN-LSTM

This model is a hybrid 1D CNN-LSTM network designed to extract both local and sequential features from spectral data. Initially, the input spectra are processed by a 1D convolutional block consisting of two convolutional layers with 16 and 32 filters, respectively, small kernel sizes, batch normalization, ReLU activations, and dropout to prevent overfitting, with max-pooling applied after each layer to reduce dimensionality. The extracted feature sequences are then passed to an LSTM layer with 32 hidden units, which captures temporal dependencies across the spectral sequence, followed by dropout for regularization. Finally, a fully connected classifier maps the learned sequential features to the output classes through a dense layer of 32 neurons with ReLU activation, followed by a dropout layer, and a softmax output layer corresponding to the number of rice classes. The network is trained using the Adam optimizer with weight decay, minimizing categorical cross-entropy loss, and employs early stopping and learning rate reduction to improve generalization, effectively combining local spectral feature extraction with sequential modeling while controlling overfitting.

Experimental Setting

The dataset was partitioned into three subsets: training (70%) for model development, validation (15%) for hyperparameter tuning, and testing (15%) for final performance evaluation. This partitioning ensured methodological rigor and prevented data leakage.

To ensure generalizability and mitigate overfitting, hyperparameter optimization was conducted via a systematic grid search. The validation set performance served as the primary criterion for model selection, with the final parameter configurations determined by optimizing validation accuracy to maintain an optimal bias-variance trade-off.

The models' performance was evaluated on the held-out test set using comprehensive metrics, including accuracy, precision, recall, and F1-score. The training process was monitored using loss curves, and a confusion matrix was generated to provide a detailed visualization of the classification performance across all rice varieties.

Classical models were trained in two configurations: (1) using extracted handcrafted features and (2) using the reduced spectral dataset comprising every 20th band. In contrast, deep learning models were trained exclusively on the reduced sequential data to leverage their capacity

for end-to-end learning from spectral sequences. This dual approach enabled a comprehensive evaluation of feature engineering versus learned representations in rice variety classification.

RESULTS AND DISCUSSION

The initial experiment involved training five classical classifiers using 27 extracted features as input. The performance of these models on the test set is summarized in Table 1. The SVM classifier achieved the highest accuracy (86.07%), followed by MLR (82.55%). In contrast, the DT classifier exhibited the lowest performance among all models, with 69.8% accuracy. Analysis of the confusion matrices presented in Figure 7 reveals that the most frequent misclassification occurred between the Domsiyah and Alikazemi varieties, suggesting a higher spectral similarity between these two classes.

Subsequently, the impact of using the sequential information from spectral profiles directly—rather than handcrafted features—was investigated. To address the high dimensionality of the raw spectral data, every 20th spectral band was selected for down sampling. This preprocessed data was then used to train the same five classical classifiers, in addition to the deep learning models. The performance comparison across the four rice varieties using this down sampling approach is detailed in Table 2. Figures 8 and 9 present the confusion matrices for the classical and deep learning models, respectively.

The results show that the accuracy of SVM increased substantially to 92.62%, and MLR's accuracy rose to 88.26%. Notably, the performance of RF, DT, and GB classifiers did not change significantly with the new input features. This can be attributed to the nature of the algorithms; Tree-based models (RF, DT, and GB) treat each spectral band independently and do not explicitly model wavelength-order relationships, so they failed to capitalize on the spectral shape information present in the raw data. In contrast, SVM and MLR can exploit correlation between adjacent bands (via regularization or kernel similarity), allowing them to capture the smooth spectral profiles and thus achieve higher accuracy.

The one-layer LSTM and two-layer LSTM models achieved high accuracies of 88.76% and 89.00%, respectively. The 1D-CNN model attained 84.23% accuracy, while the hybrid CNN-LSTM model reached 87.42%. Training progress for the deep learning models—including training and validation accuracy, as well as training and validation loss—is illustrated in Figures 10–13, confirming the absence of overfitting. Although these deep learning models demonstrated strong performance, they were outperformed by the SVM classifier, suggesting that SVM's kernel-based discrimination was more effective for this task than the sequential modeling of LSTM networks.

Table 1. Performance comparison of classifiers across four rice varieties using 27 extracted features as input.

Classifier	Accuracy (%)	Precision (%)	Recall (%)	F1-score (%)
SVM	86.07	86.18	86.07	86.10
RF	79.19	78.79	79.19	78.93
MLR	82.55	82.38	82.55	82.45
DT	69.80	70.11	69.80	69.95
GB	81.38	81.39	81.38	81.35

Table 2. Performance comparison of classifiers across four rice varieties using reduced spectral data (every 20th band) as input.

Classifier	Accuracy (%)	Precision (%)	Recall (%)	F1-score (%)
SVM	92.62	92.59	92.62	92.58
RF	80.70	80.34	80.70	80.32
MLR	88.26	88.14	88.26	88.19
DT	69.97	69.95	69.97	69.97
GB	81.54	81.25	81.54	81.22
1D-CNN	84.23	84.18	84.23	83.90
LSTM (1-Layer)	88.76	88.94	88.76	88.72
LSTM (2-Layer)	89.00	89.00	88.00	88.00
CNN-LSTM	87.42	87.74	87.42	87.50

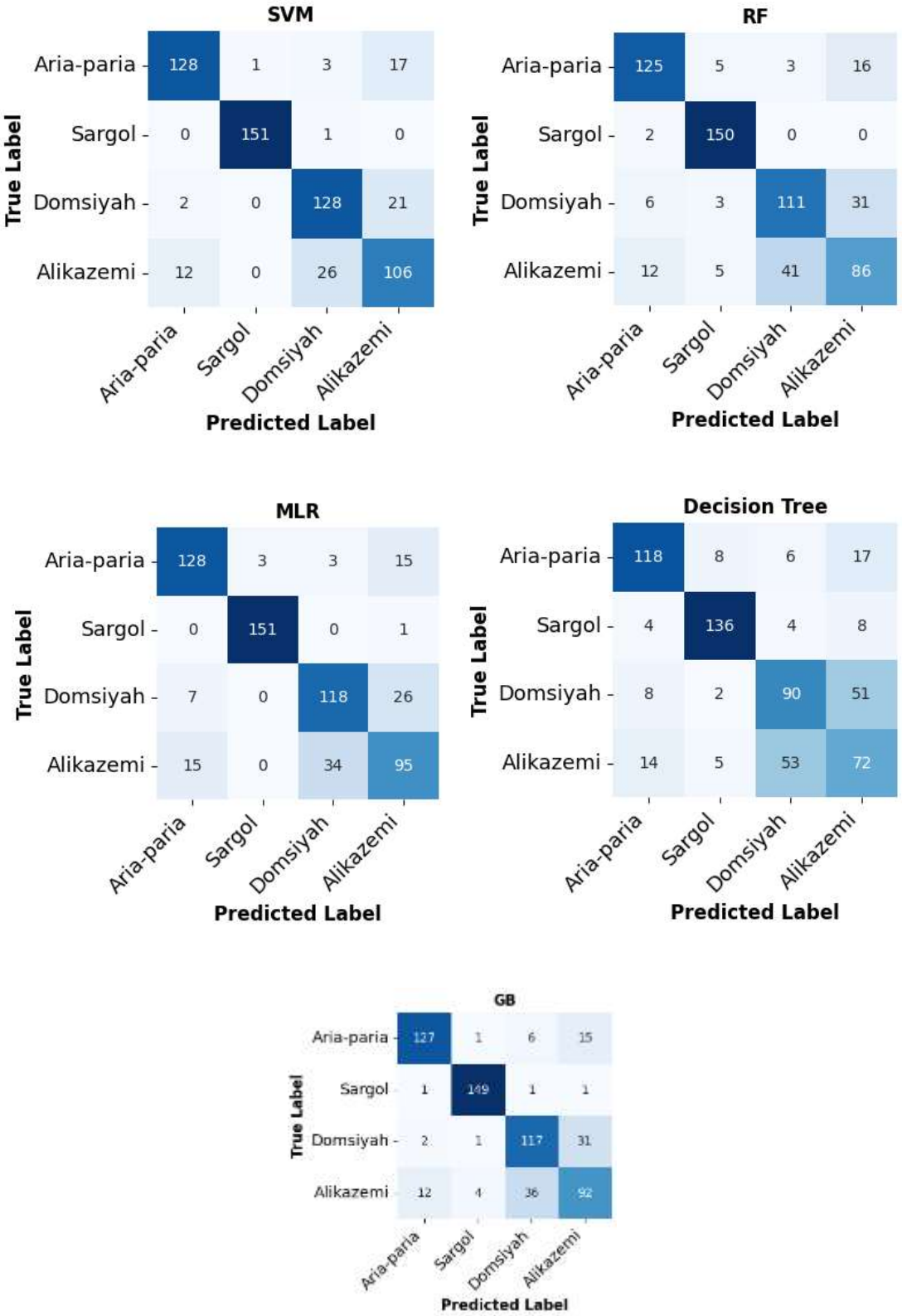

Figure 7. Confusion matrices of the classic classifiers across four rice varieties using 27 extracted features as input.

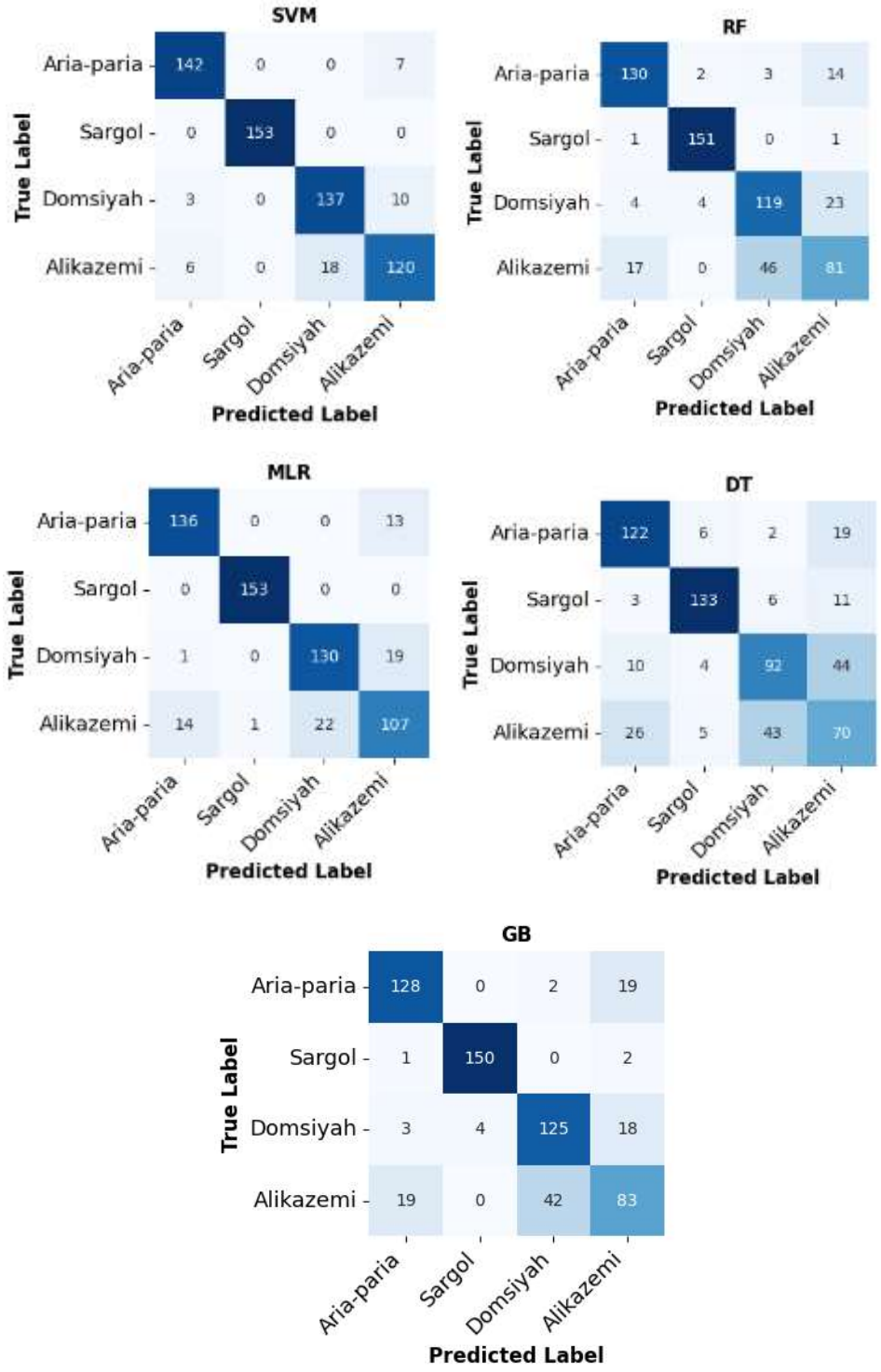

Figure 8. Confusion matrices of the classic classifiers across four rice varieties using reduced spectral data (every 20th band) as input.

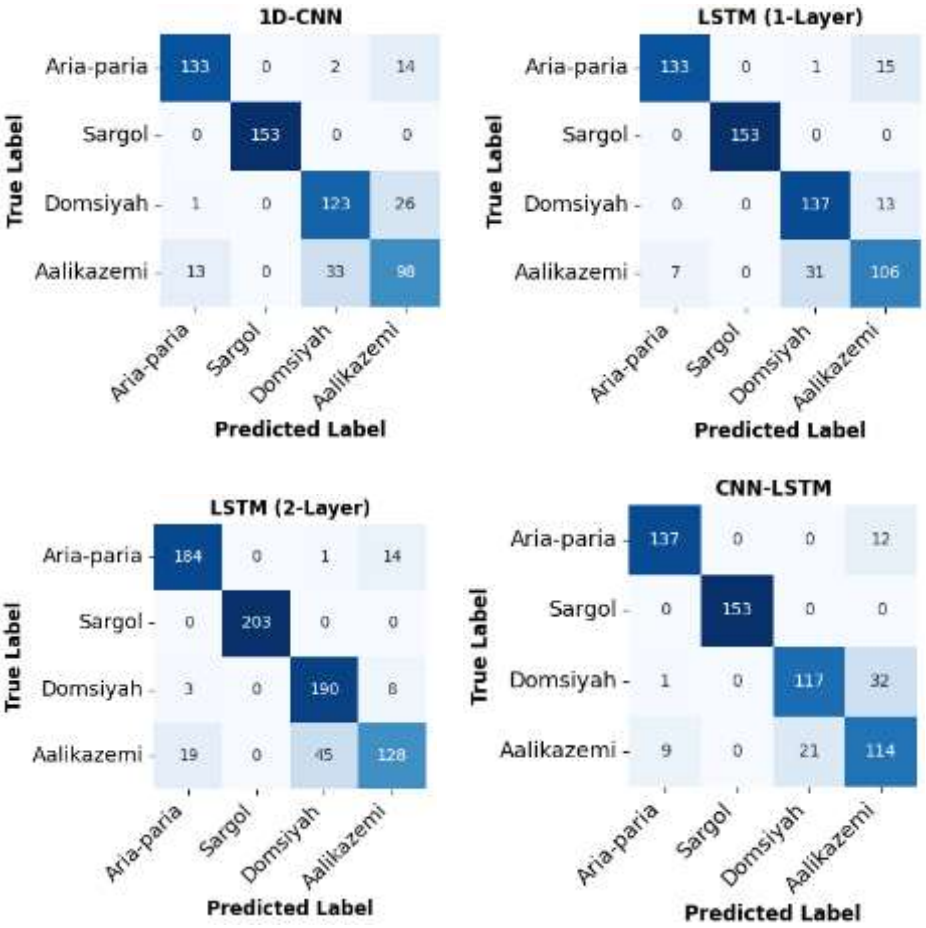

Figure 9. Confusion matrices of the deep models across four rice varieties using reduced spectral data (every 20th band) as input.

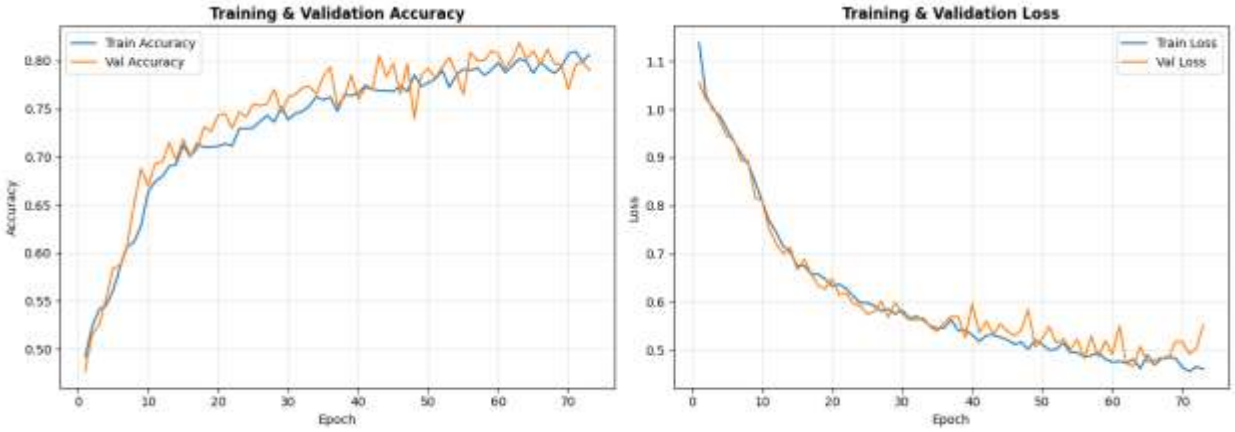

Figure 10. Training progress of the one-dimensional convolutional neural network across four rice varieties using reduced spectral data (every 20th band) as input.

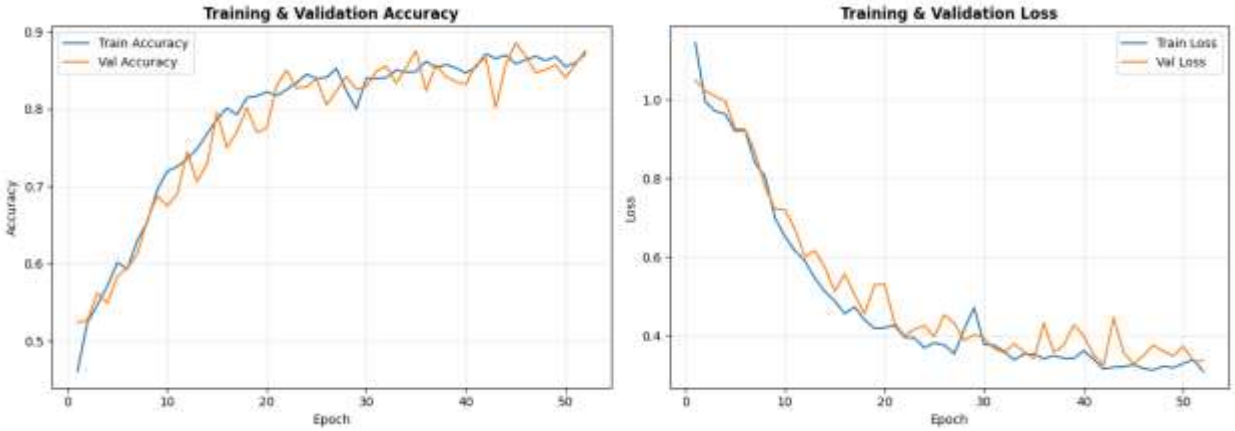

Figure 11. Training progress of the long short-term memory network (1-Layer) across four rice varieties using reduced spectral data (every 20th band) as input.

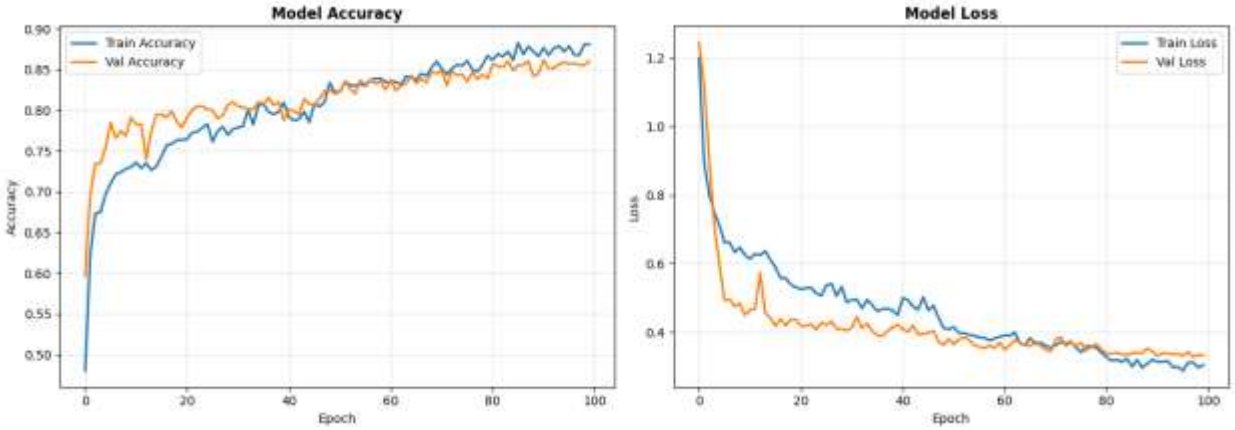

Figure 12. Training progress of the long short-term memory network (2-Layer) across four rice varieties using reduced spectral data (every 20th band) as input.

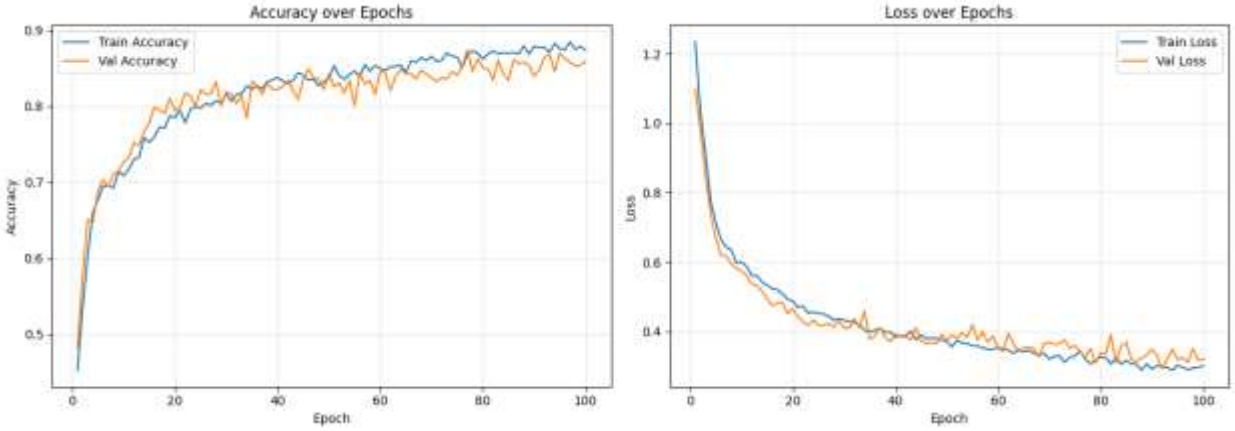

Figure 13. Training progress of the stacked one-dimensional convolutional neural network and long short-term memory network across four rice varieties using reduced spectral data (every 20th band) as input.

In this study, hyperspectral images of four rice varieties were acquired using a hyperspectral imaging system with anisotropic spatial sampling, providing a spatial resolution of 0.2 mm in the scanning direction and 1 mm in the cross-direction over a 10 × 20 cm area. This anisotropy caused rice grains aligned with the scan direction to appear as compressed, while tilted grains were represented as elongated or thin structures that were often removed during segmentation.

To compensate for this disparity and improve grain detection, images were resized from 472 × 200 to 472 × 1000 pixels (5:1 ratio), achieving isotropic resolution (0.2 mm per pixel in both directions). This enhancement enabled better delineation of tilted/displaced grains and complete grain boundaries. This improvement was validated visually. Without resizing, tilted rice grains were undetectable and discarded during segmentation, reducing the dataset from more than 4000 total grains to only 3,181. Resizing enabled complete recovery of all grains for analysis.

The original spectral resolution (~0.5 nm) was down sampled to approximately 10 nm (20× reduction). Rather than relying solely on feature extraction methods such as PCA, spectral down sampling was adopted to investigate the minimum spectral resolution suitable for industrial deployment, where processing speed and real-time analysis are critical. Many industrial hyperspectral imaging systems operate at spectral resolutions of 5 nm or higher, and reducing data dimensionality directly lowers computational complexity and hardware requirements while preserving physical wavelength interpretability.

Compared to previous studies on rice variety classification—which often rely on high spectral resolution hyperspectral data and dataset-specific feature extraction methods such as PCA—this work evaluates classification performance under more practical, application-oriented imaging conditions. By uniformly down sampling the spectral resolution to 10 nm, this study demonstrates that reliable classification remains achievable while significantly reducing data dimensionality, which is critical for real-time and industrial implementations. Unlike PCA-based representations, the proposed approach preserves uniform wavelength spacing and physical interpretability, providing a realistic simulation of lower-resolution hyperspectral cameras. Furthermore, addressing the anisotropic spatial resolution inherent to line-scan imaging systems improves grain segmentation and data completeness—an aspect often overlooked in related works. Overall, this study provides complementary insights to the existing literature by emphasizing practical constraints and model performance trade-offs rather than solely maximizing classification accuracy under ideal laboratory conditions.

The 20× spectral down-sampling strategy led to a substantial improvement in classification performance for several models, most notably the SVM classifier, whose accuracy increased from 86.07% using handcrafted features to 92.62% when sequential spectral information was directly exploited. A similar performance gain was observed for MLR, with accuracy rising from 82.55% to 88.26%, indicating that preserving spectral order enhances class separability. In contrast, the performance of tree-based classifiers remained largely unchanged. This suggests that the additional spectral shape information captured by the down-sampled sequential features provided minimal new discriminative power for these particular models. While tree-based models can capture complex interactions through hierarchical splits, they treat each spectral band as an independent feature and do not inherently impose a smoothness constraint or weight relationships based on wavelength adjacency. Consequently, they are less efficient at exploiting the continuous, correlated structure of spectral data when it is encoded as individual, highly collinear features, compared to methods like SVM or regularized linear models that can learn from the global geometric structure of the feature space.

Confusion matrix analysis revealed that Alikazemi and Domsiyah exhibited the highest

misclassification rates, likely due to spectral signature similarity. In contrast, Sargol achieved superior classification performance, attributable to its distinctly higher spectral reflectance compared to other varieties. The results from different classifiers (Table 2) indicate that the 2-layer LSTM (89.00% accuracy) offers no significant improvement over the 1-layer LSTM (88.76%), despite having ~7× more parameters (281,510 vs. 39,988). The 1D-CNN and CNN-LSTM models had 8,868 and 11,398 parameters, respectively. Among deep models, the 2-layer LSTM ranked highest, followed by the 1-layer LSTM.

Furthermore, although deep learning models (1D-CNN, LSTM, and CNN–LSTM) were designed to capture local and long-range spectral dependencies, their performance did not surpass that of SVM on the down-sampled spectra. This outcome may be attributed to the limited size of the dataset, which can restrict the ability of deep architectures to learn complex spectral patterns effectively.

Although SVM achieved the highest accuracy with substantially fewer parameters and greater complexity compared to deep learning alternatives—making it preferable for industrial classification of these specific rice varieties—its scope is limited to the four varieties on which it was trained. Generalizing the system to classify new, unseen varieties would require retraining on an expanded dataset that includes them. It is important to note that for the defined four-class problem, SVM demonstrated excellent generalization with no signs of overfitting, as evidenced by closely matched performance across training, validation, and test sets—a robustness shared by all classical classifiers in this study.

CONCLUSIONS

This study demonstrates that accurate rice variety classification can be achieved using aggressively down sampled hyperspectral data (~10 nm spectral resolution), supporting the feasibility of real-time industrial deployment where computational efficiency is critical. Among the evaluated methods, classical classifiers—particularly SVM—outperformed deep learning models, achieving a maximum accuracy of 92.62% while requiring substantially fewer parameters. This highlights the effectiveness of kernel-based discrimination for hyperspectral rice classification tasks.

Uniform spectral down sampling preserved wavelength-specific interpretability, while spatial resolution correction enabled complete grain recovery from line-scan imaging constraints. The greatest classification confusion occurred between the Alikazemi and Domsiyah varieties due to their spectral similarity, whereas the Sargol variety exhibited the highest discriminability.

Overall, the 20× spectral reduction maintained high classification performance while approximating the spectral resolution of industrial hyperspectral imaging systems (≥5 nm). These findings indicate that aggressive spectral reduction can retain—and in some cases enhance—discriminative information while significantly reducing data dimensionality. The consistent superiority of SVM, combined with its computational efficiency and reduced susceptibility to overfitting, positions it as a strong candidate for edge-based food quality inspection systems. This work therefore shifts emphasis from laboratory-level accuracy maximization toward deployment-oriented performance trade-offs.

Future research should validate the proposed approach across a broader range of rice varieties and investigate real-time implementation on embedded hardware platforms to further bridge the gap between laboratory evaluation and industrial application.

CONFLICT OF INTEREST

The authors declare no potential conflict of interest regarding the publication of this work. In addition, the ethical issues including plagiarism, informed consent, misconduct, data fabrication and, or falsification, double publication and, or

submission, and redundancy have been completely witnessed by the authors.

ACKNOWLEDGMENTS

The authors acknowledge the assistance of DeepSeek, Perplexity (Free version), and Grok in the language refinement of this manuscript. The authors would like to thank Iranian Research Organization for Science and Technology for the financial support provided under grant number of 1010804001.

REFERENCES

Ahmed, M. T., Monjur, O., Khaliduzzaman, A., & Kamruzzaman, M. (2025). A comprehensive review of deep learning-based hyperspectral image reconstruction for agri-food quality appraisal. *Artificial Intelligence Review*, *58*(4), 96. https://doi.org/10.1007/s10462-024-11090-w

Bajait, V., & Malarvizhi, N. (2024). Automated grape leaf nutrition deficiency disease detection and classification Equilibrium Optimizer with deep transfer learning model. *Network: Computation in Neural Systems*, *35*(1), 55–72. https://doi.org/10.1080/0954898X.2023.2275722

Beucher, S., & Meyer, F. (2018). The morphological approach to segmentation: the watershed transformation. In *Mathematical morphology in image processing* (pp. 433–481). CRC Press. https://doi.org/10.1201/9781482277234

Breiman, L. (2001). Random forests. *Machine learning*, *45*(1), 5–32. https://doi.org/10.1023/A:1010933404324

Breiman, L., Friedman, J., Olshen, R. A., & Stone, C. J. (2017). *Classification and regression trees*. Chapman and Hall/CRC. https://doi.org/10.1201/9781315139470

Cortes, C., & Vapnik, V. (1995). Support-vector networks. *Machine learning*, *20*(3), 273–297. https://doi.org/10.1023/A:1022627411411

Fabiyi, S. D., Vu, H., Tachtatzis, C., Murray, P., Harle, D., Dao, T. K., Andonovic, I., Ren, J., & Marshall, S. (2020). Varietal classification of rice seeds using RGB and hyperspectral images. *IEEE access*, *8*, 22493–22505. https://doi.org/10.1109/ACCESS.2020.2969847

Feng, L., Wu, B., Zhu, S., He, Y., & Zhang, C. (2021). Application of visible/infrared spectroscopy and hyperspectral imaging with machine learning techniques for identifying food varieties and geographical origins. *Frontiers in Nutrition*, *8*, 680357. https://doi.org/10.3389/fnut.2021.680357

Friedman, J. H. (2002). Stochastic gradient boosting. *Computational statistics & data analysis*, *38*(4), 367–378. https://doi.org/10.1016/S0167-9473(01)00065-2

Géron, A. (2022). *Hands-on machine learning with Scikit-Learn, Keras, and TensorFlow*. " O'Reilly Media, Inc.".

Hartigan, J. A., & Wong, M. A. (1979). Algorithm AS 136: A k-means clustering algorithm. *Journal of the royal statistical society. series c (applied statistics)*, *28*(1), 100–108. https://doi.org/10.2307/2346830

Hochreiter, S., & Schmidhuber, J. (1997). Long short-term memory. *Neural computation*, *9*(8), 1735–1780. https://doi.org/10.1162/neco.1997.9.8.1735

Jin, C., Zhou, L., Zhao, Y., Qi, H., Wu, X., & Zhang, C. (2025). Classification of rice varieties using hyperspectral imaging with multi-dimensional fusion convolutional neural networks. *Journal of Food Composition and Analysis*, *148*, 108389. https://doi.org/10.1016/j.jfca.2025.108389

Kang, Z., Fan, R., Zhan, C., Wu, Y., Lin, Y., Li, K., Qing, R., & Xu, L. (2024). The rapid non-destructive differentiation of different varieties of rice by fluorescence hyperspectral technology combined with machine learning. *Molecules*, *29*(3), 682. https://doi.org/10.3390/molecules29030682

Kiranyaz, S., Ince, T., Abdeljaber, O., Avci, O., & Gabbouj, M. (2019). 1-D convolutional neural networks for signal processing applications. ICASSP 2019-2019 IEEE International Conference on Acoustics, Speech and Signal Processing (ICASSP), (pp. 8360-8364). IEEE.

Kiratiratanapruk, K., Temniranrat, P., Sinthupinyo, W., Prempree, P., Chaitavon, K., Porntheeraphat, S., & Prasertsak, A. (2020). Development of paddy rice seed classification process using machine learning techniques for automatic grading machine. *Journal of Sensors*, *2020*(1), 7041310. https://doi.org/10.1155/2020/7041310

Komal, Sethi, G. K., & Bawa, R. K. (2022). A prototype of automatic rice variety identification system using artificial intelligence techniques. AIP Conference Proceedings, (Vol. 2455, No. 1, p. 040004). AIP Publishing LLC.

Kurniawan, R., & Sunardi, L. (2025). Integration of image enhancement technique with DenseNet201 architecture for identifying grapevine leaf disease. *MATRIK: Jurnal Manajemen, Teknik Informatika dan Rekayasa Komputer*, *24*(2), 333–346. https://doi.org/10.30812/matrik.v24i2.4137

Liu, D. C., & Nocedal, J. (1989). On the limited memory BFGS method for large scale optimization. *Mathematical programming*, *45*(1), 503–528. https://doi.org/10.1007/BF01589116

Prova, N. N. I. (2025). Enhancing agricultural research with an attention-based hybrid model for precise classification of rice varieties. *International Journal of Cognitive Computing in Engineering*, *6*, 412–430. https://doi.org/10.1016/j.ijcce.2025.02.002

Qiu, Z., Chen, J., Zhao, Y., Zhu, S., He, Y., & Zhang, C. (2018). Variety identification of single rice seed using hyperspectral imaging combined with convolutional neural network. *Applied Sciences*, *8*(2), 212. https://doi.org/10.3390/app8020212

Rao, K. R., Kim, D. N., & Hwang, J. J. (2010). *Fast Fourier transform-algorithms and applications* (Vol. 32). Springer. https://doi.org/10.1007/978-1-4020-6629-0

Rinnan, Å., Van Den Berg, F., & Engelsen, S. B. (2009). Review of the most common pre-processing techniques for near-infrared spectra. *TrAC Trends in Analytical Chemistry*, *28*(10), 1201–1222. https://doi.org/10.1016/j.trac.2009.06.007

Saber, A., Mahmoud, A., & El-Sharkawy, Y. H. (2025). Hyperspectral imaging and K-means clustering for material structure classification and detection of unmanned aerial vehicles. *Scientific Reports*, *15*(1), 31145. https://doi.org/10.1038/s41598-025-16205-z

Savitzky, A., & Golay, M. J. (1964). Smoothing and differentiation of data by simplified least squares procedures. *Analytical chemistry*, *36*(8), 1627–1639. https://doi.org/10.1021/ac60214a047

Sperandei, S. (2014). Understanding logistic regression analysis. *Biochemia medica*, *24*(1), 12–18. https://doi.org/10.11613/BM.2014.003

Zhang, A., Lipton, Z. C., Li, M., & Smola, A. J. (2023). *Dive into deep learning*. Cambridge University Press.

Zuiderveld, K. (1994). Contrast limited adaptive histogram equalization. In *Graphics gems IV* (pp. 474–485). https://doi.org/10.1016/B978-0-12-336156-1.50061-6